Infection and Immunity

Host-Nonspecific Iron Acquisition Systems and Virulence in the Zoonotic Serovar of Vibrio vulnificus

David Pajuelo, Chung-Te Lee, Francisco J. Roig, Manuel L. Lemos, Lien-I Hor and Carmen Amaro

Infect. Immun. **2014, 82(2):731. DOI: 10.1128/IAI.01117-13. Published Ahead of Print 2 December 2013.**

IAI Journals.ASM.org

Host-Nonspecific Iron Acquisition Systems and Virulence in the Zoonotic Serovar of *Vibrio vulnificus*

David Pajuelo,[a] Chung-Te Lee,[b] Francisco J. Roig,[a] Manuel L. Lemos,[c] Lien-I Hor,[b,d] Carmen Amaro[a]

Department of Microbiology and Ecology, University of Valencia, Valencia, Spain[a]; Institute of Basic Medical Sciences and Department of Microbiology and Immunology, National Cheng-Kung University, Tainan, Taiwan, Republic of China[b]; Department of Microbiology and Parasitology, Institute of Aquaculture and Faculty of Biology, University of Santiago de Compostela, Santiago de Compostela, Galicia, Spain[c]; College of Medicine, National Cheng-Kung University, Tainan, Taiwan, Republic of China[d]

The zoonotic serovar of *Vibrio vulnificus* (known as biotype 2 serovar E) is the etiological agent of human and fish vibriosis. The aim of the present work was to discover the role of the vulnibactin- and hemin-dependent iron acquisition systems in the pathogenicity of this zoonotic serovar under the hypothesis that both are host-nonspecific virulence factors. To this end, we selected three genes for three outer membrane receptors (*vuuA*, a receptor for ferric vulnibactin, and *hupA* and *hutR*, two hemin receptors), obtained single and multiple mutants as well as complemented strains, and tested them in a series of *in vitro* and *in vivo* assays, using eels and mice as animal models. The overall results confirm that *hupA* and *vuuA*, but not *hutR*, are host-nonspecific virulence genes and suggest that a third undescribed host-specific plasmid-encoded system could also be used by the zoonotic serovar in fish. *hupA* and *vuuA* were expressed in the internal organs of the animals in the first 24 h of infection, suggesting that they may be needed to achieve the population size required to trigger fatal septicemia. *vuuA* and *hupA* were sequenced in strains representative of the genetic diversity of this species, and their phylogenies were reconstructed by multilocus sequence analysis of selected housekeeping and virulence genes as a reference. Given the overall results, we suggest that both genes might form part of the core genes essential not only for disease development but also for the survival of this species in its natural reservoir, the aquatic environment.

Vibrio vulnificus is a native member of the microbiota of temperate and tropical marine ecosystems (1–5). The species is a human pathogen that causes different pathologies depending on the route of entry into the body (skin contact or injuries versus ingestion of raw seafood) and patient immune status (compromised versus noncompromised) (3, 6–10). The most severe pathology caused by *V. vulnificus* is sepsis in immunocompromised patients, either after raw seafood ingestion (primary) or after wound infection (secondary) (8, 10, 11). The mortality rate for these sepsis cases may exceed 50% (11). Interestingly, *V. vulnificus* also causes "warm-water vibriosis" in different species of aquatic animals, especially under farmed conditions (12). The most susceptible host for this vibriosis is the eel (*Anguilla anguilla* and *A. japonica*) (12). Warm-water vibriosis in its acute form is a primary sepsis, but in this case, it is triggered irrespective of the pathogen's route of entry (gills, intestine, or skin injury, etc.) and/or the host's immune status (13).

The species *V. vulnificus* is subdivided into three biotypes, among which biotype 2 (Bt2) includes the fish-virulent strains (14, 15). Recent phylogenetic studies suggest that Bt2 is a polyphyletic group, which has probably emerged in the fish-farming environment from commensal strains by the acquisition of a virulence plasmid (pVvBt2) that encodes resistance to the innate immune system of eels (and probably other teleosts) (16–19). This biotype includes a zoonotic clonal complex, designated serovar E (SerE) (17, 20, 21). Thus, *V. vulnificus* Bt2-SerE is the most suitable candidate to perform comparative fish-versus-mammal virulence studies.

Nutritional immunity, the most ancient system of defense against pathogens common to all vertebrates (22), consists of metabolic adjustments in order to make iron unavailable to microorganisms. To overcome iron starvation in host tissues, *V. vulnificus* Bt1 produces two siderophores: vulnibactin (a catechol) and an unnamed hydroxamate siderophore (23, 24). Bt1 strains use vulnibactin for scavenging iron from human transferrin (Tf) both *in vitro* and *in vivo* (in mice, the animal model for human vibriosis). Thus, Bt1 mutants deficient in vulnibactin production or in the vulnibactin receptor (VuuA) grow less efficiently in iron-deficient media and are attenuated in mouse virulence (25–27). In addition, *V. vulnificus* Bt1 can utilize non-Tf-bound iron through a heme receptor, HupA, also involved in virulence for mice (28, 29). Recently, a novel heme-specific receptor without any known role in virulence, HutR, was described in *V. vulnificus* Bt1 (30). *V. vulnificus* Bt2 seems to produce phenolates and hydroxamates and uses hemin (Hm) as the sole iron source (31, 32). The chemical nature of the siderophores as well as the role of iron acquisition systems in virulence of the zoonotic variant are unknown.

The present study is focused on the host-nonspecific iron acquisition systems used by the zoonotic serovar to infect both humans and fish. These systems are usually under Fur (ferric uptake regulator) control. Since the genome of Bt2 has not been sequenced, we identified the iron uptake genes by using a Fur titration assay (FURTA) (enables the identification of Fur-regulated genes) (33), and subsequently, we obtained single and multiple

Received 20 September 2013 **Returned for modification** 16 November 2013
Accepted 24 November 2013
Published ahead of print 2 December 2013
Editor: A. Camilli
Address correspondence to Carmen Amaro, carmen.amaro@uv.es.
Supplemental material for this article may be found at http://dx.doi.org/10.1128/IAI.01117-13.

doi:10.1128/IAI.01117-13

TABLE 1 Strains and plasmids used in this study

Strain or plasmid	Description[d]	Isolation source or reference
Strains		
V. vulnificus		
529^T	Biotype 1	Human blood (USA)[a,b]
YJ016	Biotype 1	Human blood (Taiwan)[c]
CS9133	Biotype 1	Human blood (South Korea)[b]
B2	Biotype 1	Human blood (China)[b]
MO6-24/O	Biotype 1	Diseased human (USA)[b]
CMCP6	Biotype 1	Diseased human (South Korea)[b]
94-8-119	Biotype 1	Human wound (Denmark)[b]
E64MW	Biotype 1	Human wound (USA)[b]
CG100	Biotype 1	Oyster (Taiwan)[b]
JY1305	Biotype 1	Oyster (USA)[b]
JY1701	Biotype 1	Oyster (USA)[b]
CECT4608	Biotype 1	Healthy eel (Spain)[b]
CECT4866	Biotype 2 serovar E	Human blood (Australia)[b]
CIP8190	Biotype 2 serovar E	Human blood (France)[b]
94-8-112	Biotype 2 serovar E	Human wound (Denmark)[b]
CECT5763	Biotype 2 serovar E	Eel tank water (Spain)[b]
CECT4604	Biotype 2 serovar E	Diseased eel (Spain)[b]
CECT4999	Biotype 2 serovar E	Diseased eel (Spain)[b]
CECT5198	Biotype 2 serovar A	Diseased eel (Spain)[b]
CECT5768	Biotype 2 serovar A	Diseased eel (Spain)[b]
CECT5769	Biotype 2 serovar A	Diseased eel (Spain)[b]
A11	Biotype 2 serovar A	Diseased eel (Spain)[b]
A13	Biotype 2 serovar A	Diseased eel (Spain)[b]
95-8-7	Biotype 2 serovar I	Diseased eel (Denmark)[b]
95-8-6	Biotype 2 serovar I	Diseased eel (Denmark)[b]
95-8-161	Biotype 2 serovar I	Diseased eel (Denmark)[b]
95-8-162	Biotype 2 serovar I	Diseased eel (Denmark)[b]
11028	Biotype 3	Human blood (Israel)[b]
12	Biotype 3	Human blood (Israel)[b]
Δ*hupA*	CECT4999 *hupA*-defective mutant	This study
Δ*vuuA*	CECT4999 *vuuA*-defective mutant	This study
Δ*hutR*	CECT4999 *hutR*-defective mutant	This study
Δ*hupA* Δ*vuuA*	CECT4999 *hupA vuuA*-defective double mutant	This study
Δ*hupA* Δ*hutR*	CECT4999 *hupA hutR*-defective double mutant	This study
chupA	Δ*hupA* complemented strain	This study
cvuuA	Δ*vuuA* complemented strain	This study
E. coli		
DH5α	Cloning strain	Invitrogen
H1717	*araD139* Δ*lacU169 rpsL150 relA1 flbB5301 deoC1 ptsF25 rbsR aroB fhuF*-λ placMu	74
S17-1λ*pir*	Strain containing plasmid pCVD442; *thi pro hsdR hsdM*$^+$ *recA*::RP4-2-Tc::Mu λ*pir* Km^r Nal^r	75
Plasmids		
pUC18	Cloning vector; Amp^r	Fermentas
pCVD442	Suicide vector; *sacB bla mobRP4* R6k *ori*	43
pGemT-easy	T/A cloning vector; Amp^r	Promega
pΔ*hupA*	pCVD442 with Δ*hupA* in the MCS	This study
pΔ*vuuA*	pCVD442 with Δ*vuuA* in the MCS	This study
pΔ*hutR*	pCVD442 with Δ*hutR* in the MCS	This study

[a] Type strain of the species.
[b] Strains whose published sequences were used for the phylogenetic analysis (sequences for *vvha*, *rtxA1*, *wzz*, *pilF*, *glp*, *mdh*, *pyrC*, and *pntA* were taken from references 17 and 52–56).
[c] Strain used as a reference for primer design for the *vuuA*, *hupA*, and *hutR* genes.
[d] MCS, multiple-cloning site.

mutants by allelic exchange in selected genes of strain CECT4999. The mutants and the wild-type strain were used in a series of *in vitro* and *in vivo* tests, including virulence in eels and mice, animal models for fish and human vibriosis, respectively. Finally, the evolutionary history of the identified virulence genes was inferred and compared with that of the species by multilocus sequence analysis (MLSA).

MATERIALS AND METHODS

Strains and general culture conditions. Bacterial strains (Table 1) were

routinely grown in LB-1 (Luria-Bertani broth plus 1% NaCl)/LBA-1 (Luria-Bertani agar plus 1% NaCl) or in CM9 (M9 minimal medium [34] supplemented with 0.2% Casamino Acids [Difco])/CM9A (CM9 agar) at 28°C (*V. vulnificus* Bt2-SerE) or 37°C (*Escherichia coli*) and were stored in LB-1 plus glycerol (17%) at −80°C. For FURTA (see below), the bacterial strains were grown on MacConkey agar base (Difco) supplemented with 1% lactose and 0.04 mM $FeSO_4$ (M+Fe). If necessary, ampicillin (100 μg/ml) or polymyxin B (50 U/ml) was added to the medium.

Growth in fresh blood or plasma and in artificial media supplemented with different iron sources. Fresh blood (extracted with a syringe treated with heparin [50 mg/ml in a 0.9% NaCl solution]), erythrocytes (5% [vol/vol] in PBS-1 [phosphate-buffered saline–1% NaCl, pH 7.0]), and plasma (obtained from eel and/or human blood according to methods described previously [35, 36]) were added to CM9 in a 1:1 proportion as supplements for bacterial growth. Bacteria the were grown in CM9-HP (human plasma), CM9-EP (eel plasma), CM9-HP-Fe20/200 (CM9-HP plus 20 or 200 μM $FeCl_3$), CM9-EP-Fe20/200 (CM9-EP plus 20 or 200 μM $FeCl_3$), and CM9-EE [1% eel erythrocytes plus 100 μM ethylenediamine-di-(*o*-hydroxyphenylacetic) acid (EDDA; Sigma)]. Bacteria were also grown in CM9-Fe (CM9 plus 100 μM $FeCl_3$), CM9-Hm-0.1/10 (0.1 or 10 μM bovine Hm [Sigma] plus 100 μM EDDA [Sigma]), CM9-Hb-10 (10 μM bovine hemoglobin [Sigma] plus 100 μM EDDA [Sigma]), and CM9-Tf (40 μM iron-free human apotransferrin [Sigma]).

Fresh blood and plasma as well as inactivated plasma (plasma heated at 56°C for 30 min [37] or supplemented with 100 μM $FeCl_3$ [37]) were also distributed into 96-well microtiter plates at a ratio of 100 μl per well, and100 μl of a bacterial suspension in PBS-1 containing 10^3 CFU/ml was then added to each well. The plates were incubated at 28°C (eel) or 37°C (human) with shaking (200 rpm) for 24 h. Bacterial counts on plates of tryptone soy agar plus 1% NaCl (TSA-1) were performed by the drop plate method at 0, 4, and 24 h of incubation.

Siderophore detection. The chrome azurol S (CAS) assay was used to detect siderophore production in the supernatant of iron-restricted cultures (38). The Arnow phenolic acid assay and the Csàky hydroxylamine hydroxamic acid assay were carried out to detect phenolic- and hydroxamic-type siderophores, respectively, as previously described (39, 40). *Vibrio anguillarum* strain RV22 and *Photobacterium damselae* subsp. *damselae* strain CECT626^T were used as positive controls for the Arnow and Csàky tests, respectively (31).

Fur titration assay. The Fur titration assay (FURTA) is based on multiple plasmid-encoded Fur boxes derepressing chromosomal Fur-regulated genes by titrating the Fur protein (33). FURTA was performed according to methods described previously (33). Total DNA from *V. vulnificus* strain CECT4999 was extracted and partially digested by using the frequent-cut restriction enzyme Sau3AI, and the 0.5- to 6-kb fragments were cloned into the BamHI site of pT7-7 and transformed into *E. coli* DH5α (Table 1). DNA from a pool of 5,000 colonies was extracted and transformed by electroporation in *E. coli* H1717 on M+Fe, where Fur-regulated promoters were identified as red transformants.

Isolation of mutant and complemented strains. The general procedures for DNA extraction and manipulation were performed according methods described previously (41). Single and multiple in-frame mutants were obtained by allelic exchange (42). Briefly, a series of plasmids was created in pCVD442 (a suicide vector that allows negative selection by sucrose) (43) by cloning fragments that contained the upstream and downstream regions of each gene with an in-frame deletion of the major part of the coding sequence (Table 1). Plasmids pΔhupA, pΔvuuA, and pΔhutR, containing the up- and downstream regions of *hupA*, *vuuA*, and *hutR*, respectively, were transferred by conjugation from *E. coli* S17-1λ*pir* into wild-type strain CECT4999 to obtain single mutants. To obtain double mutants, the corresponding plasmids were transferred by conjugation into the corresponding single mutants (Table 1). Transconjugants were subsequently selected with 10% sucrose from those having lost pCVD442 via a second homologous recombination event. Complemented *chupA* and *cvuuA* strains were generated by conjugal transfer of the wild-type genes, obtained with primer pair hupA-cF/hupA-cR or vuuA-cF/vuuA-cR, cloned into pGEMT (19) (Table 1). Table 2 shows all the primers, which were designed from the published genome sequences of *V. vulnificus* strain YJ016.

***In vitro* characterization of mutants. (i) Tf bioassay.** The ability to use iron from iron-saturated human Tf (holo-Tf; Sigma) was assayed by measuring the growth halo around Tf discs (soaked in a solution of 1 mM holo-Tf) placed onto CM9A-E (CM9–100 μM EDDA) plates previously inoculated with 100 μl of a culture grown overnight in CM9.

(ii) Hm bioassay. The ability to use Hm as the sole iron source was tested by measuring bacterial growth (optical density at 600 nm [OD_{600}]) in CM9-Hm-1 at 1-h intervals during 10 h, with a final measurement at 24 h (32). Tubes were inoculated with a culture grown overnight in CM9 (1/100, vol/vol) and were incubated at 28°C with shaking (200 rpm).

(iii) Outer membrane protein analysis. Strains were grown in CM9-Fe and CM9-Tf for 12 h, and outer membrane proteins (OMPs) were extracted as described previously (44). OMP samples were fractionated by sodium dodecyl sulfate-polyacrylamide gel electrophoresis (SDS-PAGE) according to the method of Laemmli (45), using a separation gel of 10% acrylamide. The protein bands were stained with Coomassie brilliant blue.

***In vivo* phenotypic characterization of mutants.** All the protocols were reviewed and approved by the Animal Ethic Committee of the University of Valencia.

(i) Animal maintenance. Three populations of farmed European eel (*Anguilla anguilla*) of 10 g, 20 g, and 100 g were used for virulence assays, colonization assays, and blood extraction, respectively. The eels were purchased from a local eel farm that does not vaccinate against *V. vulnificus*. Fish were placed in quarantine into 170-liter tanks (6 fish of 100 g, 12 of 20 g, or 20 of 10 g per tank) containing brackish water (1.5% NaCl, pH 7.6) with aeration, filtration, and feeding systems at 25°C for a week. After quarantine, healthy fish were distributed into 100-liter tanks at the same ratio, infected with *V. vulnificus* (13), and maintained for 1 week under the same maintenance conditions but without feeding. Six- to eight-week-old BALB/c mice were purchased from Harlan Laboratory Models S.L. and maintained for 48 h in 100-liter plastic cages with water and feed supplied by the animal housing facilities of the University of Valencia.

(ii) Virulence. For eels, virulence was determined after immersion or intraperitoneal (i.p.) injection according to methods described previously (13). Mice were preinjected with iron (Hm [2.8 μg/g of mouse], $FeCl_3$ [9 μg/g of mouse], or Hm plus $FeCl_3$ [1.4 μg of Hm/g of mouse plus 4.5 μg of $FeCl_3$/g of mouse]) 2 h before challenge, and virulence was determined after i.p. injection according to methods described previously (35). For both eels and mice, a total of six animals were used per control, strain, and dose and were maintained in independent cages or tanks (13, 35). Animal mortality was recorded for 1 week and was considered only if the inoculated bacterium was reisolated in pure culture from the moribund animal. Virulence (50% lethal dose [LD_{50}]) was calculated according to the method of Reed and Muench (46) and was expressed as CFU/g (i.p. injection) or ml of infective bath (immersion challenge).

(iii) Colonization. A total of 24 eels per strain were bath infected according to methods described previously (13), with a bacterial dose corresponding to the LD_{50} of the wild-type strain, and 6 were immersed under the same conditions in PBS-1 (control). Twelve live eels were then randomly sampled at 0, 9, 24, and 72 h, at a ratio of 3 eels per sampling point (47, 48). Samples for bacterial counting on TSA-1 were taken from blood, head kidney, liver, spleen, and gills according to methods described previously (48), and bacterial counts were expressed as CFU/ml (blood) or CFU/g.

RNA isolation and quantitative reverse transcription-PCR (qRT-PCR). Total RNA from bacterial cultures in the mid-log phase or from infected eel tissues was prepared with Tri reagent (Sigma). RNA extractions were subjected twice to DNase treatment with Turbo DNase (Ambion), extending the reaction time up to 45 min at 37°C. To clean the Turbo DNase reaction mixtures and concentrate RNA, samples were sub-

TABLE 2 Primers used in this study

Primer	Restriction site	Sequence	Product size (bp)	Utilization
hupA-1	SphI	CGGCATGCCAGTAAGAATCCATTAGAGG	1,401	Mutant construction
hupA-2	KpnI	CGGGTACCCGTGATTTAACTCAAGCAG		Mutant construction
hupA-3	KpnI	CGGGTACCATCTTGAGCTTGTACTGG	1,407	Mutant construction
hupA-4	SphI	CGGCATGCGTCCTGATGAATAAGATC		Mutant construction
vuuA-1	SalI	CGGTCGACATTCCTACACTTAGCCGC	1,404	Mutant construction
vuuA-2	KpnI	CGGGTACCCTAAAACAGCAACCACGT		Mutant construction
vuuA-3	KpnI	CGGGTACCCCCCATCACTACCGCAGAC	1,401	Mutant construction
vuuA-4	SacI	CGGAGCTCTCCGTGATGATATTGCTAAG		Mutant construction
hutR-1	SalI	GCGTCGACTATGCCGCCAGTGATGCAAA	1,435	Mutant construction
hutR-2	PstI	GCCTGCAGGTTGGCAGCGAGTACCGAC		Mutant construction
hutR-3	PstI	GCCTGCAGACTTATTCCACAGAGCCGGGG	1,423	Mutant construction
hutR-4	SphI	GCGCATGCCCATACATACCTTGCAAAACG		Mutant construction
hupA-cF		TTAGAAGTTGTATTTCACAC	2,366	Mutant complementation
hupA-cR		TTTAACTCCTTTGGTGATC		Mutant complementation
vuuA-cF		CTAGAAGTTCAACTGCAATG	2,407	Mutant complementation
vuuA-cR		AGGCATCTCATGCGGTGAG		Mutant complementation
hupA-seq1		GAATGAGACTTAAAAAGCC	1,001	Sequencing
hupA-seq2		CCTGATGCGAAGGAAATGA		Sequencing
hupA-seq3		TCATAACGAACACCAGGAG	964	Sequencing
hupA-seq4		CAGCCAGGCGTGTTTGAT		Sequencing
hupA-seq5		CATATCCGGATCAACCGTGA	500	Sequencing
hupA-seq6		GGAACGACATAAGAGCCAT		Sequencing
vuuA-seq1		CTCTGGTCAACATCAGAGGC	1,122	Sequencing
vuuA-seq2		ATGATCGATACACTAATCCG		Sequencing
vuuA-seq3		AACTCTTTACCTTCAGTGG	1,101	Sequencing
vuuA-seq4		CATCCTGAATGCAATCAG		Sequencing
hutR seq-1		GGACAGGCGTAAAGGATTGG	1,229	Sequencing
hutR seq-2		GACGCTCAGACGTTCTCGAA		Sequencing
hutR seq-3		TGCTGATATGACCAAGGCG	1,231	Sequencing
hutR seq-4		TGCTGTACTTGCTCGACGC		Sequencing
recA-F		CGCCAAAGGCAGAAATCG	59	qRT-PCR
recA-R		ACGAGCTTGAAGACCCATGTG		qRT-PCR
hutR-qF		CATGGCGGATGTTGAAGATATC	76	qRT-PCR
hutR-qR		AACTGCGTTTTTGCTCCGTAA		qRT-PCR
hupA-qF		AAGCTAGATGCTGCGCCTTT	60	qRT-PCR
hupA-qR		CACGGTTGATCCGGATATGC		qRT-PCR
vuuA-qF		GGACCACGGGAATCCATATG	56	qRT-PCR
vuuA-qR		TGCGTTGGCGGGTTTTA		qRT-PCR

jected to a cleaning step by using the RNeasy MinEute Cleanup kit (Qiagen). RNA was quantified with a Biophotometer (Eppendorf) and used to obtain cDNA by using Moloney murine leukemia virus (M-MLV) reverse transcriptase (Invitrogen). For each reaction, 1 μg of total purified RNA was used. Quantification of cDNA by quantitative PCR (qPCR) was performed with Power SYBR green PCR Master Mix (Applied Biosystems) with a StepOne Plus RT-PCR system (Applied Biosystems). The threshold cycle (C_T) values were determined with StepOne software V2.0 (Applied Biosystems), to establish the relative RNA levels of the tested genes. Primers specific to *recA* (recA-F/recA-R), *hutR* (hutR-qF/hutR-qR), *hupA* (hupA-qF/hupA-qR), and *vuuA* (vuuA-qF/vuuA-qR) were used to amplify DNA fragments of about 60 to 70 bp (Table 2). DNA denaturing was conducted from 60°C to 95°C to obtain the melting curve for determining the PCR amplification specificity. For each tested gene, three independent bacterial cultures were subjected to RNA extraction and cDNA isolation, and for each one, three measurements of cDNA were performed. The housekeeping gene *recA* was used as a standard, and the fold induction ($2^{-\Delta\Delta CT}$) for each gene was calculated according to methods described previously (49).

DNA isolation and sequencing. Genomic DNA was extracted, according to the miniprep protocol for genomic DNA extraction (50), from a selection of *V. vulnificus* strains representative of the genetic and phenotypic variability of the species (Table 1). Primers were designed from the genome of *V. vulnificus* YJ016 by using vector NTI 9.1.0 (Table 2). PCR was performed in a 20-μl reaction volume that contained 0.2 μM forward and reverse primers, 1.5 U of *Taq* DNA polymerase (GoTaq, 5 U/μl; Promega), 4 μl of 5× *Taq* reaction buffer (GoTaq Green; Promega), 0.5 mM $MgCl_2$, 0.1 mM deoxynucleoside triphosphate (dNTP) mix (Promega), and 2 μl of DNA. PCR was performed in a Techne thermocycler (TC-412). The reaction started with 10 min of denaturation at 94°C, which was followed by 35 cycles of 40 s of denaturation at 94°C, 45 s of annealing at 50°C to 54°C, and 45 s of extension at 72°C. An additional extension step at 72°C for 10 min completed the reaction. Amplicons were examined by agarose gel electrophoresis (1%) and ethidium bromide staining. PCR products of the predicted size were purified and sequenced in an ABI 3730 sequencer (Applied Biosystems).

Phylogenetic analysis. The evolutionary scenario of *vuuA* and *hupA* was evaluated from the whole sequence of each gene and was compared with an MLSA reconstruction (51) from the partial sequences (254 nucleotides [nt] by gene) of four virulence-associated genes (*vvha*, *rtxA1*, *wzz*, and *pilF*) and four housekeeping genes (*glp*, *mdh*, *pyrC*, and *pntA*) taken from GenBank (17, 52–56). Phylogenetic trees for each single gene and for the concatenated MLSA were obtained by using the maximum likelihood (ML) method with PhyML software (57). The best evolutionary model for

TABLE 3 Virulence, siderophore production, and growth in serum and with holo-Tf as the sole iron source[e]

Strain	Virulence (LD_{50})[a]			Siderophore production result[b]			Growth in fresh serum from[c]:		
	Mice (CFU/mouse)	Eels							
		i.p. (CFU/eel)	Bath (CFU/ml)	Arnow	Csàky	CAS	Humans	Eels	Mean growth (mm) with holo-Tf ± SD[d]
CECT4999	3.16×10^2	2.1×10^2	4.4×10^6	+	−	+	151.3	141.26	17.3 ± 2.8
Δ*vuuA*	4.01×10^3	1.0×10^4	$>10^8$	+	−	+	5.68	9.55	0
Δ*hupA*	8.97×10^3	1.7×10^4	$>10^8$	+	−	+	4.02	3.23	ND
Δ*hutR*	3.2×10^2	2.0×10^2	5×10^6	+	−	+	ND	ND	ND
cvuuA	ND	6.2×10^2	4.1×10^6	+	−	+	80.2	165.5	16.3 ± 2.8
chupA	ND	5.7×10^2	5.6×10^6	+	−	+	178.1	108.6	ND
Δ*vuuA* Δ*hupA*	$>10^7$	7.4×10^5	$>10^8$	+	−	+	3.73	4.8	ND

[a] The LD_{50} for mice was determined by using the iron-overloaded model (35). The LD_{50} is expressed as CFU per fish or mouse in the case of i.p. injection and CFU per ml in the case of bath infection of eels (13).
[b] Criteria for positive or negative results for each test according to reference 31.
[c] Ratio between final and initial bacterial counts on TSA-1 plates after 4 h of incubation in fresh serum.
[d] Diameter of growth halo in mm around Tf discs (soaked in a solution of 1 mM holo-Tf) placed onto CM9A-E plates previously inoculated with 100 μl of a culture grown overnight in CM9.
[e] ND, not done.

the sequences according to jModelTest (58) and considering the Akaike information criterion (AIC) (59) was found to be the Tamura 3-parameter model (T92 model) (60) for the *vuuA* and *hupA* genes and for the MLSA-concatenated alignment. The model was applied with a gamma distribution and invariant sites accounting for heterogeneity in evolutionary rates among sites. Support for the groupings derived in these reconstructions was evaluated by bootstrapping using 1,000 replicates. No outgroups were used for the analysis of both genes due to the huge interspecies differences. The congruence among phylogenetic reconstructions obtained with the different alignments was checked by using Shimodaira-Hasegawa (SH) (61) and expected-likelihood weight (ELW) tests as implemented in TreePuzzle, version 5.2 (62, 63).

Molecular clock estimation for *vuuA* and *hupA*. The following equation was used to roughly determine the age of divergence for each pairwise comparison: number of synonymous single-nucleotide polymorphisms (sSNPs)/(number of sSNP sites × mutation rate × number of generations per year) (64). The sSNPs were selected because they are believed to be neutral or nearly neutral in terms of selection and therefore allow for a relatively unbiased estimation of SNP accumulation (64). The number of potential sSNP sites for each codon was calculated from a lookup table of codon possibilities and added together to give the number of potential sSNP sites for all the codons in the sequence. Since the synonymous mutation rate of *V. vulnificus* is unknown, we selected a value of 1.4×10^{-10} mutations per base pair per generation based on mutation rate data from *E. coli* (65). The generation times *in vitro* for *V. vulnificus* biotypes 1, 2, and 3 are 4.0, 2.9, and 2.4 generations h^{-1}, respectively (66). However, there are no data on generation time in the environment. On the basis of the estimations performed for *E. coli* (100 to 300 generations/year) (67), *Bacillus anthracis* (43 generations per year) (68), and *Vibrio parahaemolyticus* (100 generations per year) (69), we chose a value of 365 generations per year for *V. vulnificus*.

Statistical analysis. All the experiments were performed in triplicate, and significance of the differences was tested by using the unpaired Student *t* test with a *P* value of <0.05.

Nucleotide sequence accession numbers. Sequences for *hupA*, *vuuA*, and *hutR* were deposited into GenBank under accession numbers KC741503, KC741545, and KF056337.

RESULTS

FURTA and siderophore assays. The open reading frames (ORFs) with significant homology to *V. vulnificus* Bt1 genes identified by FURTA are shown in Table S1 in the supplemental material. The set includes chromosomal genes such as the genes for the receptors HupA (clone DP006) and VuuA (clone DP009) (but not for the receptor HutR), for vulnibactin and heme transport, and for vulnibactin biosynthesis as well as a plasmid gene of unknown function (see Table S1 in the supplemental material). No gene related to hydroxamate-type siderophore biosynthesis could be identified, although a cluster of genes for exogenous aerobactin utilization was found (see Table S1 in the supplemental material). Accordingly, the strain was positive in the CAS assay, a universal assay for siderophore detection; positive in the test for phenolates; and negative in the test for hydroxamates (Table 3).

Isolation and characterization of the single and multiple mutants. (i) Fur box and sequencing. Clones DP006 and DP009 were sequenced, and two fur boxes with the sequences GCTAATGAT AATTACTATC and GCAAAGCATTCTCATTTGC, highly similar to those identified previously by Litwin and Byrne (28) in *hupA* (identical) and by Webster and Litwin (27) in *vuuA* (18/19), were identified. In parallel, *hupA* and *vuuA*, together with *hutR* (selected despite not being identified by FURTA), were sequenced in strain CECT4999 (Table 1), using primers from the genome sequence of Bt1 strain YJ016 (Table 2). The *hupA*, *vuuA*, and *hutR* genes showed 97%, 95%, and 97% similarity values (in amino acid sequence) with respect to the homologous ones in Bt1 strain YJ016, respectively.

(ii) Transcription versus iron starvation. A positive fold induction for the three genes was observed *in vitro* when bacteria were subjected to the iron-restricted conditions imposed by apo-Tf (Fig. 1A). In the case of genes for Hm receptors, the transcription level of *hupA* was significantly higher than that of *hutR* (Fig. 1A). A positive fold induction of *vuuA* and *hupA* was also detected when fresh plasma from either humans or eels was added to CM9 (Fig. 1A). This positive stimulation of gene transcription of *vuuA* and *hupA* was abolished when $FeCl_3$ was added to plasma at concentrations of 20 μM and 200 μM, respectively, which suggests that transcription of *vuuA* is more sensitive to iron concentrations.

(iii) OMP profiles and siderophore production. According to data described previously (27, 28), the OMP profiles of Δ*hupA* and Δ*vuuA* strains lack proteins of 77 and 72 kDa, respectively, which were present in the OMP profiles of the wild-type strain and the complemented strains (Fig. 2). No difference in protein profile

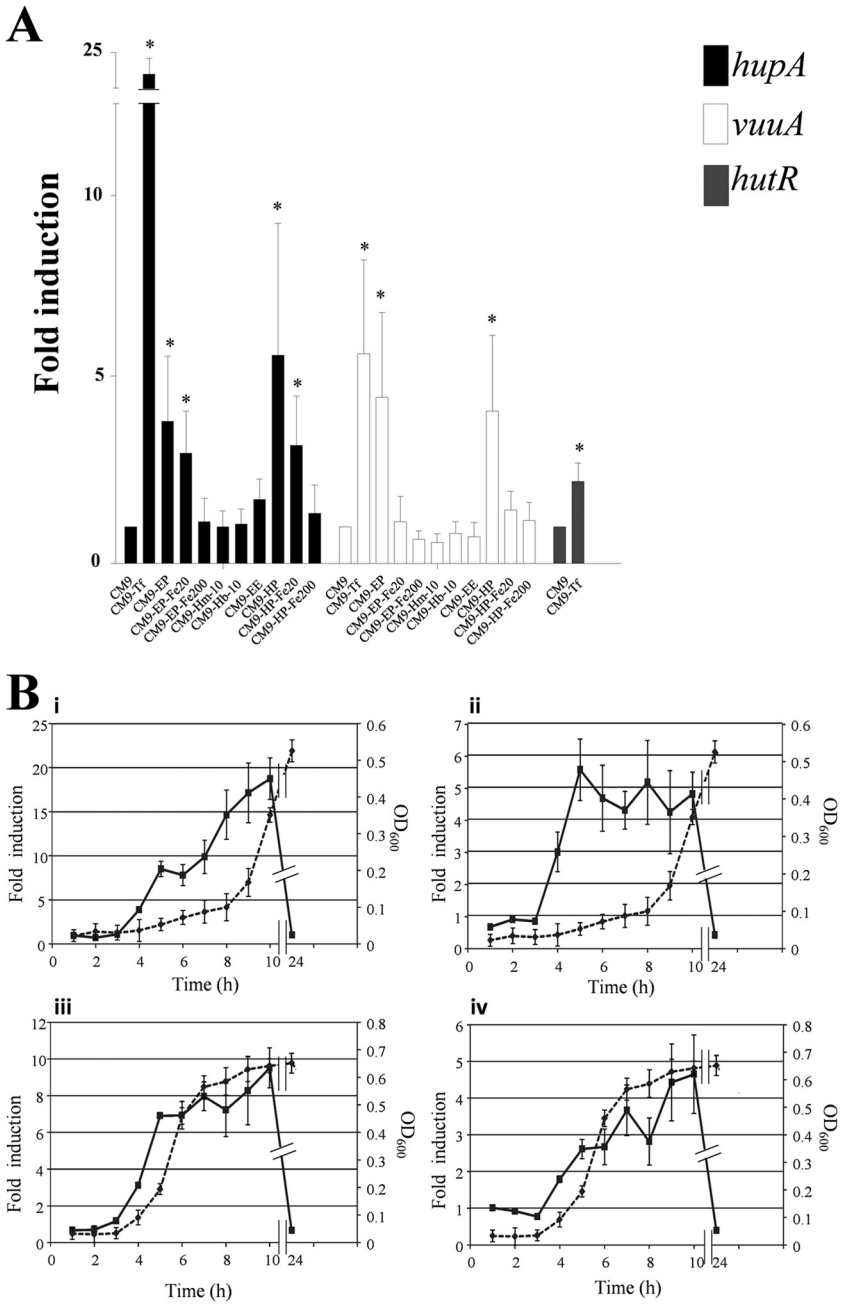

FIG 1 Effect of iron starvation on transcription of *hutR*, *hupA*, and *vuuA*. (A) Transcription of the *hutR*, *hupA*, and *vuuA* genes was measured by qRT-PCR in the mid-log phase of growth for CM9 (control), iron-free CM9 (CM9 plus 100 μM EDDA) supplemented with different iron sources (1% eel erythrocytes [CM9-EE], 10 μM bovine hemin [CM9-Hm-10], or 10 μM bovine hemoglobin [CM9-Hb-10]), and iron-free CM9 (CM9 plus plasma [CM9-EP or CM9-HP] supplemented with 20 or 200 μM $FeCl_3$ [CM9-EP-Fe20, CM9-EP-Fe200, CM9-HP-Fe20, or CM9-HP-Fe200]). (B) Time course analysis of *hupA* (i and iii) and *vuuA* (ii and iv) transcription in CM9-Tf (i and ii) and CM9-EP (iii and iv) measured by qRT-PCR (continuous line) versus bacterial growth (dashed line). Asterisks denote significant differences ($P < 0.05$) compared with the control conditions (CM9).

was apparent when OMP of the Δ*hutR* strain was compared with those of the wild-type and the complemented strains (data not shown). As expected, none of the mutations affected the ability to produce siderophores (Table 3).

(iv) Utilization of iron from holo-Tf and Hm. The Δ*vuuA* strain was unable to use iron from holo-Tf (Table 3), while the Δ*hupA* and Δ*hutR* strains grew with Hm as the sole iron source but with different growth patterns (Fig. 3). Thus, the Δ*hupA* strain grew significantly less than the wild-type strain and showed a retarded log phase, while the Δ*hutR* strain grew as efficiently as the wild-type strain (Fig. 3). A *hupA hutR* double mutant was constructed as described in Materials and Methods. The double mutant was unable to grow with Hm as the only iron source (Fig. 3). In all cases, the complemented strains presented the wild-type phenotype (Table 3 and Fig. 3).

(v) Virulence for mice and eels. The *hupA* and *vuuA* single

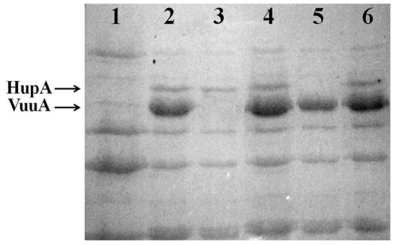

FIG 2 OMP profiles obtained by SDS-PAGE. Lane 1, CECT4999 in CM9-Fe; lane 2, CECT4999 in CM9-Tf; lane 3, the Δ*vuuA* strain in CM9-Tf; lane 4, the c*vuuA* strain in CM9-Tf; lane 5, the Δ*hupA* strain in CM9-Tf; lane 6, the *chupA* strain in CM9-Tf. Arrows indicate bands of 72 and 77 kDa.

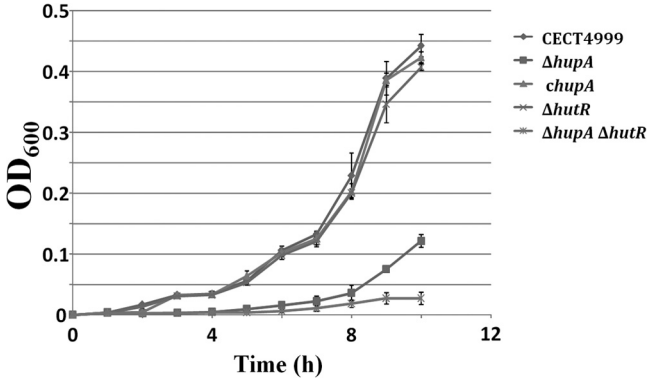

FIG 3 Growth of *V. vulnificus* strains with hemin as the sole iron source (CM9-Hm-0.1). Cultures of CECT4999, the Δ*hupA* and Δ*hupR* single mutants, the Δ*hupA* Δ*hupR* double mutant, and the *chupA* strain grown overnight were used to inoculate (1:100, vol/vol) CM9-Hm-0.1 (0.1 μM hemin plus 100 μM EDDA), and the OD_{600} was measured at 1-h intervals for 10 h, with a final reading at 24 h postinoculation.

mutants showed a similar increase in the LD_{50} values in both animal models (between 1 and 2 log units) (Table 3). Surprisingly, both mutants were completely avirulent when they were administered to eels through water, which is the natural route of vibriosis transmission (Table 3). In contrast, the *hutR* single mutant was as virulent as the wild-type strain in both animal models (Table 3), and as a consequence, it was excluded from subsequent experiments.

A *hupA vuuA* double mutant was found to be completely avirulent for mice and almost avirulent for i.p. injected eels (Table 3). As expected, the double mutant was avirulent for eels infected through water. Finally, the complemented strains exhibited the wild-type level of virulence for eels and mice (Table 3).

Colonization and invasion assays. (i) *In vivo* assays. To discover whether *vuuA* and/or *hupA* plays a role in host colonization and/or invasion (spreading and colonization of the internal organs), the well-established eel model was selected (48). The two single mutants were able to colonize the gills and establish a population with a size similar to that of the wild-type strain (Fig. 4A). From this location, the single mutants spread to the internal organs, where they survived <72 h postchallenge (Fig. 4A). No significant difference in the degree of colonization of internal organs was detected between the Δ*hupA* and Δ*vuuA* strains, although the Δ*hupA* strain spread faster in blood. Finally, the double mutant was able to colonize the gills but failed to spread to internal organs (data not shown).

In parallel, samples of internal and external organs from eels infected with the wild-type strain were processed to determine whether both genes were induced during the infection process. As observed in Fig. 4B, overexpression of genes was not induced in gills at any of the assayed times but was significantly induced in blood at 9 h and in all the internal organs sampled at 24 h (except for *vuuA*, which was not induced in head kidney) but became undetectable at 72 h postchallenge.

(ii) *In vitro* assay. Single and double mutants were able to survive and grow in fresh eel plasma and human plasma although at significantly lower rates than the wild-type and the complemented strains (Table 3 and Fig. 5). Interestingly, the growth of each strain did not vary significantly with regard to the tested condition (blood versus plasma or human versus eel) (Fig. 5), and therefore, EP was the condition selected to demonstrate that the reduction in the growth rate was due to the bacteriostatic effect of Tf and not to the bacteriolytic action of complement. As expected, significant differences in bacterial growth between each mutant and the wild-type strain were still found after complement inactivation but not after iron supplementation (Fig. 5). Finally, the complemented strains showed a growth rate similar to that of the wild-type strain under all assayed conditions (Fig. 5).

To relate growth rate and gene expression, we studied the fold induction of *hupA* and *vuuA* versus the growth of the wild-type strain under iron-restriction conditions (apo-Tf for fresh EP). As shown in Fig. 1B, transcription of both genes was induced just before the early log phase and was maintained for 10 h, indicating that both genes are expressed before the utilization of HupA and VuuA as iron receptors for active growth.

Phylogeny of *vuuA* and *hupA*. The *vuuA* and *hupA* genes were sequenced for a collection of *V. vulnificus* strains from clinical and environmental sources belonging to the three biotypes and the three previously defined phylogroups (17) (GenBank accession numbers KC741503 to KC741545 and KF056337).The phylogenetic reconstruction using the maximum likelihood (ML) method showed that the *vuuA* gene has two main variants (Fig. 6): *vuuA* variant I [*vuuA(I)*] is present in 26 of the 29 studied strains, including sequenced strain YJ016 (of Bt1 and of clinical origin) and all the Bt2 and Bt3 strains, and *vuuA(II)* is present in a few environmental and clinical Bt1 strains, including sequenced strain CMCP6 (54). The intervariant identity in both DNA and protein sequences is around 80 to 85%, while the intravariant identity is between 89.7 and 90.3% for *vuuA(I)* and between 97.7 and 98.1% for *vuuA(II)*. The *hupA* gene also presents two main variants (Fig. 6): *hupA(I)* was found in all strains from diseased fish and clinical cases associated with fish manipulation; *hupA(II)* also has two subforms, one defective because it lacks a fragment of 2,035 nt in the 5′ portion of the gene [*hupA(IIa)*] and the other complete [*hupA(IIb)*] (Fig. 6). The intervariant identity in both DNA and protein sequences was between 91.6 and 95.6%, while the intravariant identities were from 96.1 to 95.9% for *hupA(I)* and 95 to 95.1% for *hupA(II)*, being 100% for *hupA(IIa)* and between 95 and 95.1% for *hupA(IIb)*. The sequences of both genes were compared to identify the regions where the mutations accumulated. As shown in Tables S2 and S3 in the supplemental material, variations were detected throughout the protein. Meanwhile, *vuuA* presented changes in 156 amino acids (63.5% amino acids of different families and 36.5% amino acids of the same family), while *hupA* showed variations in 41 amino acids (68.3% amino acids of different families and 31.7% amino acids of the same family).

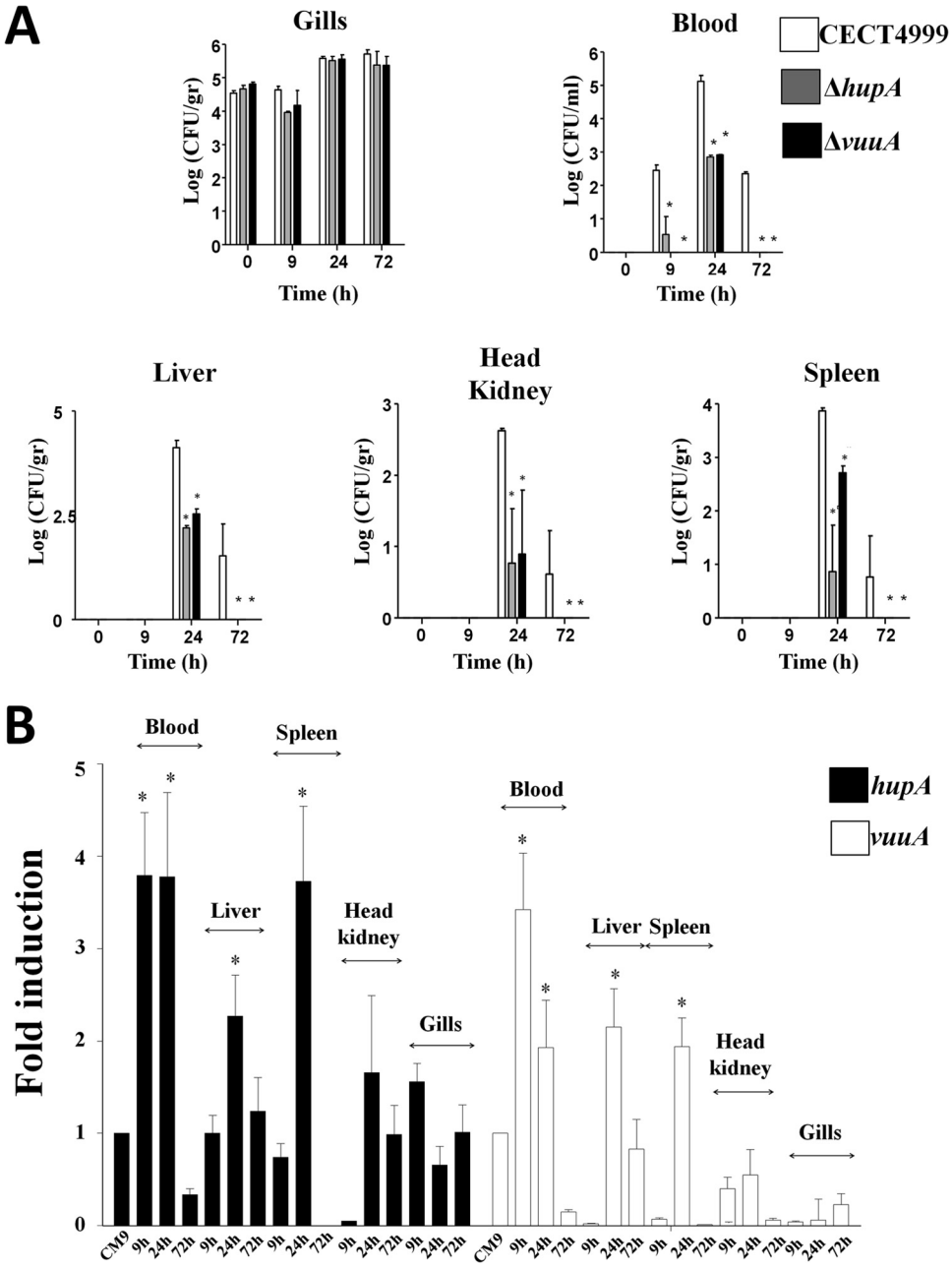

FIG 4 Eel colonization and invasion assays and *in vivo* gene overexpression. (A) Eels were bath infected with the wild-type strain (CECT4999) or with each one of the single mutants (Δ*hupA* or Δ*vuuA*) at a dose of 10^6 CFU/ml for 1 h. The degree of bacterial colonization of external (gills) and internal (blood, liver, head kidney, and spleen) organs was then measured as bacterial counts (CFU per g or ml) at 0, 9, 24, and 72 h postchallenge. Asterisks indicate significant differences in bacteria recovered from mutant strain- and wild-type strain-infected eels ($P < 0.05$). (B) Eels were bath infected with the wild-type strain (CECT4999) at a dose of 10^6 CFU/ml for 1 h, and gene expression levels of *vuuA* and *hupA* were determined in external (gills) and internal (blood, liver, head kidney, and spleen) organs by qRT-PCR at 0, 9, 24, and 72 h postchallenge. Asterisks indicate significant induction of each gene with respect to the expression level in CM9 ($P < 0.05$).

The phylogenetic trees for each gene were compared with that obtained by MLSA from the selected housekeeping and virulence-related genes to discover whether their phylogenetic histories were congruent with one another. Figure 6 shows the MLSA tree for the species obtained from the concatenated selected genes (housekeeping [*glp*, *mdh*, *pyrC*, and *pntA*] and virulence related [*vvha*, *rtxA1*, *wzz*, and *pilF*]), together with the trees obtained for *vuuA* and *hupA*. The results of the Shimodaira-Hasegawa (SH) and expected-likelihood weight (ELW) tests are summarized in Table 4. All the comparisons were highly significant for both tests, which indicates that the phylogenetic reconstructions obtained from each single gene (*vuuA* or *hupA*) are congruent with one another and with the species tree, thus providing statistical support for similar evolutionary rates. In other words, the evolutionary history of *vuuA* and *hupA* does not differ significantly from that of the species inferred from the MLSA of the selected housekeeping

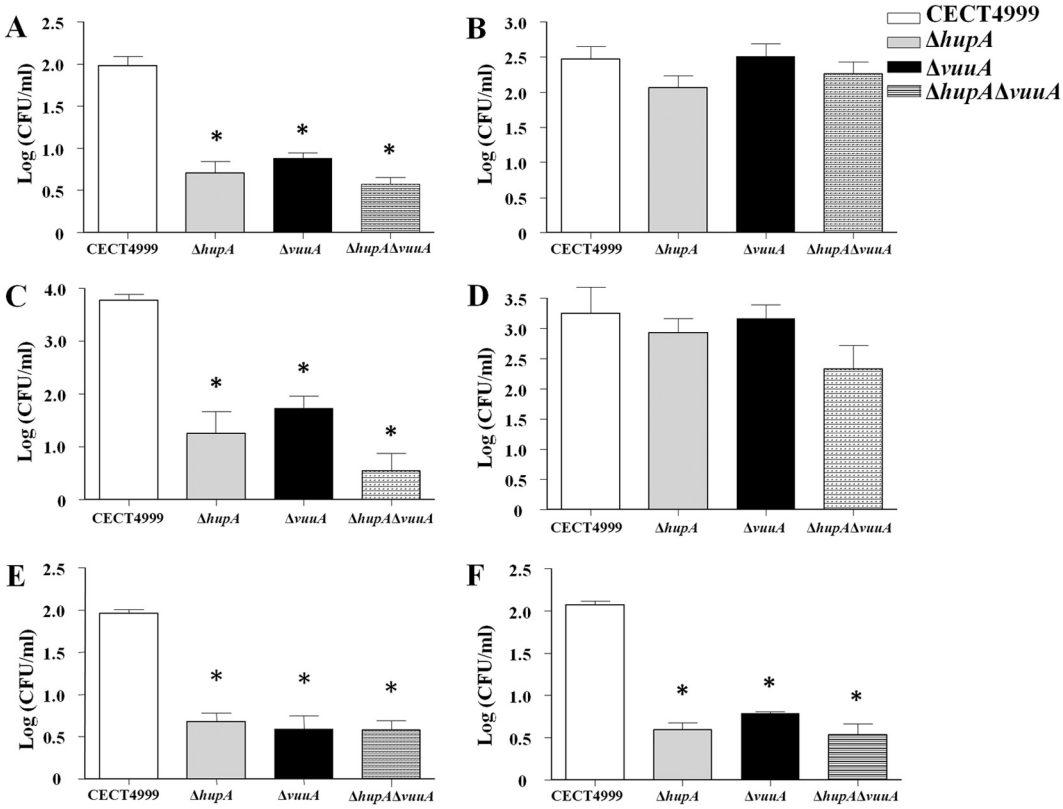

FIG 5 Growth in plasma and blood. Bacterial growth of *V. vulnificus* strains in plasma and blood is presented as an increase of CFU/ml, expressed as $\log_{10}$ units, after 4 h of incubation. (A) Fresh eel plasma (EP); (B) EP plus 200 μM $FeCl_3$; (C) heat-inactivated EP; (D) heat-inactivated EP plus 200 μM$FeCl_3$; (E) eel blood; (F) human plasma. Asterisks indicate significant differences in growth between the mutant and wild-type strains ($P < 0.05$).

and virulence-related genes, all of them belonging to the core genes.

We also estimated the time of divergence by using sSNPs (64). The number of sSNPs for the *hupA* gene ranged from 0 to 86, with an average of 22 sSNPs/strain. In the case of *vuuA* type I, the average number of sSNPs was 49/strain (ranging from 0 to 119), and for type II, the average number was 21/strain (ranging from 16 to 26). The potential numbers of sSNP sites were 2,047 for *hupA* and 2,018 and 1,962 for *vuuA* types I and II, respectively. These numbers were used to calculate the molecular clock, the results of which are shown in Tables 5 to 7. According to the model used, based on *E. coli* (365 generations per year and a mutation rate of 5.4×10^{-10}), Bt1 strains diverged from each other an average of 55,000 years ago, regardless of the considered gene, whereas strains within the other groups diverged from 0 years ago (Bt3) to 20,000 years ago (Bt2) in the case of *hupA* and from 0 years ago (Bt3) to 73,000 years ago (Bt2) in the case of *vuuA*.

DISCUSSION

The present work focused on the host-nonspecific iron acquisition systems, believed to be chromosomal, that the zoonotic serovar of *V. vulnificus* employs to infect both humans and fish. To do so, mice and eels were chosen as animal models to test the role that these mechanisms play in virulence. Previous studies on the iron uptake mechanisms of *V. vulnificus* Bt2, and in particular the zoonotic variant, suggest that it is able to produce phenolate- and hydroxamate-type siderophores and to use Hm as the sole iron source (31, 32). On the basis of siderophore production by Bt1 strains, it was hypothesized that Bt2 strains produce vulnibactin and a new hydroxamate-type siderophore (31). The genes for biosynthesis and uptake of vulnibactin were identified by FURTA, but no gene related to hydroxamate production was detected. This finding was further confirmed by performing specific tests for siderophore detection, which were positive only for phenolate production. Thus, the selected strain of the zoonotic serovar produces only vulnibactin, demonstrating that there are differences in siderophore production among strains of the same clonal complex. Additional identified genes were those related to exogenous aerobactin uptake, previously identified in Bt1 of the species (70), as well as those related to Hm uptake, which would constitute the genetic basis for this previously reported ability (32).

The hypothesis of the present study is that the iron uptake systems from vulnibactin and Hm are host-nonspecific virulence factors. The selected genes (*vuuA*, *hupA*, and *hutR*) were sequenced, and the corresponding proteins showed a similarity value of >95% with regard to the clinical Bt1 strain used as a reference. The single mutants and corresponding complemented strains were obtained by allelic exchange and were phenotypically evaluated in terms of siderophore production, OMP profiles, and growth in the presence of holo-Tf or Hm as the sole iron source. In general terms, the phenotype obtained was the expected one. Thus, vulnibactin production was not affected by any of the three mutations, the OMP profiles from Δ*vuuA* and Δ*hupA* strains lacked the corresponding predicted band, and the Δ*vuuA* strain

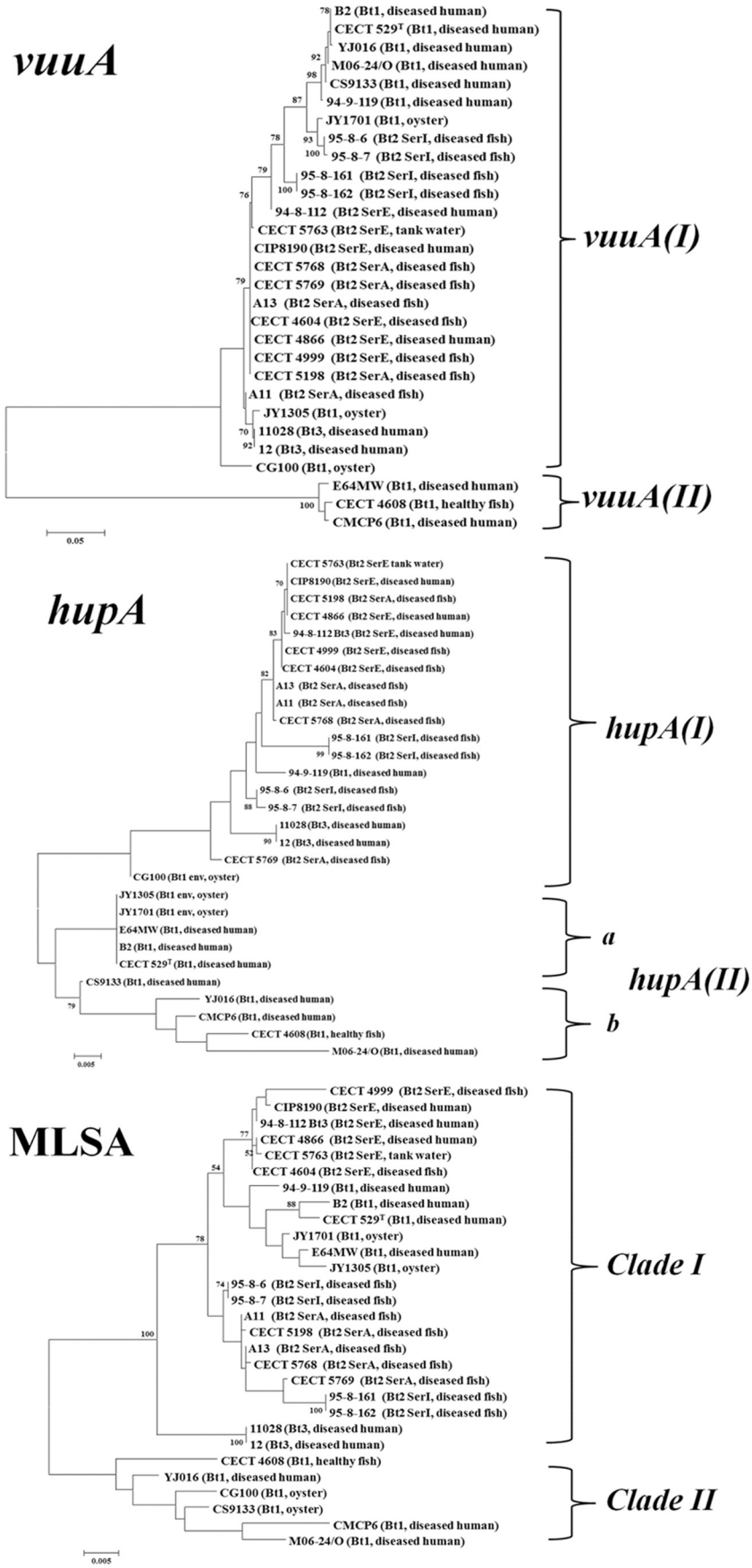

FIG 6 Phylogenetic trees. The maximum likelihood tree was derived from the *vuuA* and *hupA* genes and MLSA by the T92 model using a discrete Gamma distribution plus assuming that a certain fraction of sites are evolutionarily invariable. Bootstrap support values of >70% are indicated in the corresponding nodes.

TABLE 4 Summary of Shimodaira-Hasegawa and expected-likelihood weights for the MLSA sequences and *vuuA* and *hupA* genes

Alignment	Topology	lnL[a]	Probability value[b]	
			SH test	ELW test
MLSA	MLSA	−7,732.85	1.000	1.000
	vuuA	−6,246.04	1.000	0.0056
	hupA	−7,757.89	1.000	0.9589
vuuA	*vuuA*	−4,970.60	1.000	0.6663
	MLSA	−4,347.71	1.000	0.1373
	hupA	−4,539.55	1.000	0.4489
hupA	*hupA*	−4,553.87	1.000	0.0289
	vuuA	−4,842.49	1.000	1.000
	MLSA	−4,717.26	1.000	0.9205

[a] Each alignment was used to evaluate the log likelihood (lnL) of the ML tree obtained with each of the three data sets.
[b] The probability values for each topology and test are shown. All the values were in the 0.95 confidence test.

was unable to grow in the presence of holo-Tf as the sole iron source. With respect to *hutR*, we did not detect differences in OMP profiles between the mutant and wild-type strains, which correlates with the results obtained by Datta and Crosa (30), who suggested that HutR is a minority protein in the outer membrane. Regarding iron uptake from Hm, we found that *hupA* is the gene mainly involved in this system, since its disruption significantly diminished the ability to grow with Hm as the sole iron source. However, *hutR* is also needed to completely abolish growth ability *in vitro*. This result is also compatible with those obtained by Datta and Crosa (30), who suggested that *hutR* plays a secondary role in the use of Hm by *V. vulnificus* Bt1. In parallel, we confirmed that the three genes were induced under iron restriction conditions and that *hupA* was expressed at a significantly higher level than *hutR*, a result again in concordance with the hypothesis that *hutR* is secondary in Hm uptake. The finding that *vuuA* and *hupA* were maximally induced in the log phase of growth suggests that they are probably involved in active growth both *in vivo* and *in vitro*. Finally, the complemented strains showed the phenotype of the wild-type strain, demonstrating that in each case, the mutation affected only the target gene(s).

The results obtained in the virulence assays support the hypothesis on the role of *hupA* and *vuuA* as host-nonspecific virulence genes. Thus, in single-gene (*hupA* or *vuuA*) knockout mutants, virulence was attenuated by 1 to 2 logs for both i.p. injected eels and mice, while virulence was completely abolished for eels when bacteria were administered by water, the natural route for vibriosis transmission. In contrast, *hutR* was found not to be a virulence gene since its mutation did not affect the lethal dose for either animal model. This result is compatible with those obtained *in vitro* and also supports the hypothesis posed by Datta and Crosa (30). Interestingly, the double-gene (*hupA* and *vuuA*) knockout mutant was completely avirulent for mice and almost avirulent for eels, both inoculated by the i.p. route, suggesting that iron acquisition by either ferric vulnibactin or heme uptake is essential for the zoonotic serovar to cause sepsis in both mice and eels. The fact that virulence of the double mutant (*vuuA* and *hupA*) was not completely abolished for eels suggests that the zoonotic strain may employ a third iron acquisition system, which is probably host specific. In fact, one of the genes identified by FURTA was a plasmid gene, *vep20*, previously annotated as a putative receptor for Tf (16) on the basis of its low similarity with a gene encoding a putative Tf receptor in *Histophilus somni*, one of the key bacterial pathogens involved in the multifactorial etiology of the bovine respiratory disease complex (71). A BLASTP search revealed that the highest homology for this protein is in a series of putative Tf/Hb-binding proteins in various human and fish pathogens (*Vibrio harveyi*, *Photobacterium damselae*, *Neisseria meningitidis*, and *Bordetella* sp.). pVvBt2 contains a system that enables the bacterium to survive the innate immune system of teleosts (18; our unpublished results). One of the genes involved, namely, *vep07*, encodes an outer membrane lipoprotein that confers resistance to fish serum activated by the alternative route (C.-T. Lee, D. Pajuelo, C. Amaro, and L. Hor, unpublished data). Our unpublished data suggest that another gene in pVvBt2, *vep20*, probably encodes a host-specific receptor for Tf involved in the phenotype of resistance to the innate immune system of teleosts. Further studies are under way to test this hypothesis.

On the basis that *vuuA* and *hupA* are virulence genes, the next step was to discover their specific roles in human and fish vibriosis. To this end, we performed a series of *in vivo* and *in vitro* experiments under the hypothesis that this pathogen needs both genes to grow in host blood and internal organs and to achieve the popu-

TABLE 5 Average time of divergence for the *hupA* gene based on sSNP analysis, taking 365 generations per year and a mutation rate of 5.4×10^{-10}

Biotype	Avg time of divergence (yr) for *hupA*				
	Bt1	Bt2-SerE	Bt2-SerI	Bt2-SerA	Bt3
Bt1	55,295.0	63,173.2	61,476.6	61,786.4	74,710.2
Bt2-SerE	63,173.2	1,321.9	19,828.3	6,237.7	29,329.4
Bt2-SerI	61,476.6	19,828.3	20,447.9	19,518.5	29,432.6
Bt2-SerA	61,786.4	6,237.7	19,518.5	8,303.1	26,768.2
Bt3	74,710.2	29,329.4	29,432.6	26,768.2	0.0

TABLE 6 Average time of divergence for *vuuA* type I based on sSNP analysis, taking 365 generations per year and a mutation rate of 5.4×10^{-10}

Biotype	Avg time of divergence (yr) for *vuuA* type I				
	Bt1	SerE	SerI	SerA	Bt3
Bt1	56,847.9	85,458.0	65,612.5	89,392.2	93,163.4
Bt2-SerE	85,458.0	13,744.1	73,067.7	9,134.8	31,007.9
Bt2-SerI	65,612.5	73,067.7	42,950.2	79,195.9	7,416.6
Bt2-SerA	89,392.2	9,134.8	79,195.9	4,022.6	21,873.2
Bt3	93,163.4	31,007.9	74,167.6	21,873.2	0.0

TABLE 7 Average time of divergence for *vuuA* type II based on sSNP analysis, taking 365 generations per year and a mutation rate of 5.4×10^{-10}

Strain[a]	Avg time of divergence (yr) for *vuuA* type II		
	CMCP6	CECT4608	E64
CMCP6	0	20,113.2	27,655.7
CECT4608	20,113.2	0	32,684.0
E64	27,655.7	32,684.0	0

[a] All strains are of biotype 1.

lation size that triggers host death by sepsis. First, both genes were induced in eels after bath infection, which demonstrated that both genes are needed *in vivo*. The induction level of the genes was not apparently related to the bacterial numbers recovered on the plates. In fact, we were able to detect a positive induction of *vuuA* when no bacterium was recovered on the plates. This apparent contradiction is explained because vibrios could be in a VNC (viable-but-not-culturable) state, and as a consequence, the obtained counts underestimate the *in vivo* bacterial population size. In any case, the genes were induced only in internal organs (blood, spleen, and liver) and from 9 h (blood) to 24 h (blood, spleen, and liver) postinfection, which suggests that VuuA and HupA are used *in vivo* during the first 24 h of infection. After this time, cellular destruction caused by the pathogen would release iron from cellular storage depots that could be used for bacterial growth (48). This result is also compatible with a hypothesis reported previously (47), which suggests that the bacterium needs a minimum of 24 h to spread from gills to the internal organs and achieve the population size that triggers death by sepsis. We then analyzed the effect of single mutations in *vuuA* or *hupA* and that of the double mutation of both genes on surface and internal colonization of eels. We found that all the mutant strains, single and double, were able to colonize the gills as efficiently as the wild-type strain. However, each of the single mutants was deficient in internal colonization. In fact, the single mutants grew significantly less than the wild-type strain in each organ and were completely eliminated from internal organs at 72 h postinfection. This result explains why they were not virulent by bath challenge and suggests that bacterial growth inside the body is needed by *V. vulnificus* to overcome immune defenses. In addition, the double mutant strain completely lost the ability to spread from the gills to the internal organs, confirming the importance of iron acquisition by either system for colonization and invasion. Likewise, either one gene or the other was needed for efficient growth in human and eel blood and serum. In fact, both genes were induced in fresh serum from both humans and eels, which correlates with the results obtained *in vivo* and supports the hypothesis on the role played by both iron uptake systems in the ability of this zoonotic serovar to grow in blood and cause death by sepsis.

Our next step was to analyze the phylogeny of *vuuA* and *hupA* and compare it with that of the species to discover whether both genes are part of the accessory genetic elements or part of the core genes. Interestingly, the phylogenetic trees for each gene were congruent with each other and with the species constructed from the four housekeeping and four virulence-related genes. This result strongly suggests that *vuuA* and *hupA* are part of the core genes of the species and have not been acquired through horizontal gene transfer, as occurs in other pathogenic bacterial species (72). This finding also suggests that both genes probably play a role not only in virulence but also in survival outside the hosts of vibrios. Accordingly, we found two main polymorphic variants for both genes without an apparent relationship with biotype or origin (clinical versus environmental) of the isolate. However, a deeper study of the origin of the isolates provided evidence of some kind of relationship between receptor variant and environment. Thus, for *hupA*, all the strains that produced *hupA(1)* came from fish farming-related environments (diseased fish, tank water, healthy fish, and humans infected through fish handling), which suggests that *hupA* could have diverged as a consequence of better adaptation to Hm-containing fish proteins. On the other hand, in *vuuA*, this adaption to the environment was evident mainly for the zoonotic strains. In this case, the theoretical divergence time for the gene was much longer than that expected for a clonal complex. The most plausible explanation would be that the environment acts as a strong selective force because the main source of variation for this clonal complex is the multiplicity of environments from which the strains were isolated (water, healthy fish, diseased fish, human expectoration, human wound, and human sepsis). The adaptation to the environment of a siderophore receptor could be a consequence of changes in the siderophores, produced by mutations in the biosynthetic genes, due to the competence by iron in the natural environments of the bacteria. The same hypothesis was proposed to explain the variation in receptors for pyoverdin in *Pseudomonas* spp. (73). Another interesting observation provided by the phylogenetic study was that some Bt1 strains from clinical and environmental sources presented a truncated form of the *hupA* gene. Interestingly, these strains possess a whole *hutR* gene, which suggests that they could use this second receptor to take up iron from heme proteins. This finding provides a biological explanation for the presence of a second gene for the heme receptor in the genome of the species.

In conclusion, *vuuA* and *hupA* are host-nonspecific virulence genes involved in the colonization and invasion of internal organs by enabling the bacterium to grow under the iron restriction conditions imposed by mammal and teleost hosts. This work demonstrates that iron uptake is essential to cause vibriosis in mice and suggests that probably a third host-specific system could also be involved in virulence for teleosts, a hypothesis which will have to be corroborated in further studies. The phylogenetic study also suggests that both genes are part of the core genes of the species *V. vulnificus* and are subjected to variations, probably due to environmental adaptations. Finally, *hutR* encodes a secondary heme receptor that is not relevant to virulence, although it could be used by the strains with a truncated form of *hupA*, like those which we have found in this study.

ACKNOWLEDGMENTS

This work has been financed by grant AGL2011-29639 (cofunded with FEDER funds) and Programa Consolider-Ingenio 2010 grant CSD2009-00006 from the MICINN (Spain) and by grant GVACOMP2012-195 from the Conselleria de Educación Formación y Ocupación de Valencia.

We thank the SCSIE of the University of Valencia for technical support in determining sequences.

REFERENCES

1. **Arias CR, Macian MC, Aznar R, Garay E, Pujalte MJ.** 1999. Low incidence of *Vibrio vulnificus* among *Vibrio* isolates from sea water and shellfish of the western Mediterranean coast. J. Appl. Microbiol. **86:**125–134. http://dx.doi.org/10.1046/j.1365-2672.1999.00641.x.
2. **Hor LI, Gao CT, Wan L.** 1995. Isolation and characterization of *Vibrio vulnificus* inhabiting the marine environment of the southwestern area of Taiwan. J. Biomed. Sci. **2:**384–389. http://dx.doi.org/10.1007/BF02255226.
3. **Oliver JD.** 2006. *Vibrio vulnificus*, p 349–366. *In* Thompson FL, Austin B, Swings J (ed), Biology of vibrios. ASM Press, Washington, DC.
4. **Oliver JD, Warner RA, Cleland DR.** 1983. Distribution of *Vibrio vulnificus* and other lactose-fermenting vibrios in the marine environment. Appl. Environ. Microbiol. **45:**985–998.
5. **Pfeffer CS, Hite MF, Oliver JD.** 2003. Ecology of *Vibrio vulnificus* in estuarine waters of eastern North Carolina. Appl. Environ. Microbiol. **69:**3526–3531. http://dx.doi.org/10.1128/AEM.69.6.3526-3531.2003.
6. **Bullen JJ, Spalding PB, Ward CG, Gutteridge JM.** 1991. Hemochromatosis, iron and septicemia caused by *Vibrio vulnificus*. Arch. Intern. Med. **151:**1606–1609. http://dx.doi.org/10.1001/archinte.1991.00400080096018.
7. **Dalsgaard A, Frimodt-Moller N, Bruun B, Høi L, Larsen JL.** 1996.

Clinical manifestations and molecular epidemiology of *Vibrio vulnificus* infections in Denmark. Eur. J. Clin. Microbiol. Infect. Dis. **15:**227–320. http://dx.doi.org/10.1007/BF01591359.
8. **Dechet AM, Yu PA, Koram N, Painter J.** 2008. Nonfoodborne *Vibrio* infections: an important cause of morbidity and mortality in the United States, 1997-2006. Clin. Infect. Dis. **46:**970–976. http://dx.doi.org/10.1086/529148.
9. **Oliver JD.** 2005. Wound infections caused by *Vibrio vulnificus* and other marine bacteria. Epidemiol. Infect. **133:**383–391. http://dx.doi.org/10.1017/S0950268805003894.
10. **Warnock EW, MacMath TL.** 1993. Primary *Vibrio vulnificus* septicemia. J. Emerg. Med. **11:**153–156. http://dx.doi.org/10.1016/0736-4679(93)90510-E.
11. **Horseman MA, Surani S.** 2011. A comprehensive review of *Vibrio vulnificus*: an important cause of severe sepsis and skin and soft-tissue infection. Int. J. Infect. Dis. **15:**e157–e166. http://dx.doi.org/10.1016/j.ijid.2010.11.003.
12. **Austin B, Austin DA.** 1999. Bacterial fish pathogens: disease of the farmed and wild fish, 3rd ed. Springer-Praxis Publishing Ltd, Chichester, United Kingdom.
13. **Amaro C, Biosca EG, Fouz B, Alcaide E, Esteve C.** 1995. Evidence that water transmits *Vibrio vulnificus* biotype 2 infections to eels. Appl. Environ. Microbiol. **61:**1133–1137.
14. **Bisharat N, Agmon V, Finkelstein R, Raz R, Ben-Dror G, Lerner L, Soboh S, Colodner R, Cameron DN, Wykstra DL, Swerdlow DL, Farmer JJ, III, Israel Vibrio Study Group.** 1999. Clinical, epidemiological, and microbiological features of *Vibrio vulnificus* biogroup 3 causing outbreaks of wound infection and bacteraemia in Israel. Lancet **354:**1421–1424. http://dx.doi.org/10.1016/S0140-6736(99)02471-X.
15. **Tison DL, Nishibuchi M, Greenwood JD, Seidler RJ.** 1982. *Vibrio vulnificus* biogroup 2: new biogroup pathogenic for eels. Appl. Environ. Microbiol. **44:**640–646.
16. **Lee CT, Amaro C, Wu KM, Valiente E, Chang YF, Tsai SF, Chang CH, Hor LI.** 2008. A common virulence plasmid in biotype 2 *Vibrio vulnificus* and its dissemination aided by a conjugal plasmid. J. Bacteriol. **190:**1638–1648. http://dx.doi.org/10.1128/JB.01484-07.
17. **Sanjuan E, Gonzalez-Candelas F, Amaro C.** 2011. Polyphyletic origin of *Vibrio vulnificus* biotype 2 as revealed by sequence-based analysis. Appl. Environ. Microbiol. **77:**688–695. http://dx.doi.org/10.1128/AEM.01263-10.
18. **Valiente E, Lee CT, Lamas J, Hor LI, Amaro C.** 2008. Role of the virulence plasmid pR99 and the metalloprotease Vvp in resistance of *Vibrio vulnificus* serovar E to eel innate immunity. Fish Shellfish Immunol. **24:**134–141. http://dx.doi.org/10.1016/j.fsi.2007.10.007.
19. **Valiente E, Lee CT, Hor LI, Fouz B, Amaro C.** 2008. Role of the metalloprotease Vvp and the virulence plasmid pR99 of *Vibrio vulnificus* serovar E in surface colonization and fish virulence. Environ. Microbiol. **10:**328–338. http://dx.doi.org/10.1111/j.1462-2920.2007.01454.x.
20. **Amaro C, Biosca EG.** 1996. *Vibrio vulnificus* biotype 2, pathogenic for eels, is also an opportunistic pathogen for humans. Appl. Environ. Microbiol. **62:**1454–1457.
21. **Biosca EG, Oliver JD, Amaro C.** 1996. Phenotypic characterization of *Vibrio vulnificus* biotype 2, a lipopolysaccharide-based homogeneous O serogroup within *Vibrio vulnificus* species. Appl. Environ. Microbiol. **62:**918–927.
22. **Weinberg ED.** 2009. Iron availability and infection. Biochim. Biophys. Acta **1790:**600–605. http://dx.doi.org/10.1016/j.bbagen.2008.07.002.
23. **Okujo N, Saito M, Yamamoto S, Yoshida T, Miyoshi S, Shinoda S.** 1994. Structure of vulnibactin, a new polyamine-containing siderophore from *Vibrio vulnificus*. Biometals **7:**109–116.
24. **Simpson LM, Oliver JD.** 1983. Siderophore production by *Vibrio vulnificus*. Infect. Immun. **41:**644–649.
25. **Kim CM, Park RY, Park JH, Sun HY, Bai YH, Ryu PY, Kim SY, Rhee JH, Shin SH.** 2006. *Vibrio vulnificus* vulnibactin but not metalloprotease VvpE is essentially required for iron-uptake from human holotransferrin. Biol. Pharm. Bull. **29:**911–918. http://dx.doi.org/10.1248/bpb.29.911.
26. **Litwin CM, Rayback TW, Skinner J.** 1996. Role of catechol siderophore synthesis in *Vibrio vulnificus* virulence. Infect. Immun. **64:**2834–2838.
27. **Webster ACD, Litwin CM.** 2000. Cloning and characterization of *vuuA*, a gene encoding the *Vibrio vulnificus* ferric vulnibactin receptor. Infect. Immun. **68:**526–534. http://dx.doi.org/10.1128/IAI.68.2.526-534.2000.
28. **Litwin CM, Byrne BL.** 1998. Cloning and characterization of an outer membrane protein of *Vibrio vulnificus* required for heme utilization: regulation of expression and determination of the gene sequence. Infect. Immun. **66:**3134–3141.
29. **Oh MH, Lee SM, Lee DH, Choi SH.** 2009. Regulation of the *Vibrio vulnificus hupA* gene by temperature alteration and cyclic AMP receptor protein and evaluation of its role in virulence. Infect. Immun. **77:**1208–1215. http://dx.doi.org/10.1128/IAI.01006-08.
30. **Datta S, Crosa JH.** 2012. Identification and characterization of a novel outer membrane protein receptor required for hemin utilization in *Vibrio vulnificus*. Biometals **25:**275–283. http://dx.doi.org/10.1007/s10534-011-9501-y.
31. **Biosca EG, Fouz B, Alcaide E, Amaro C.** 1996. Siderophore-mediated iron acquisition mechanisms in *Vibrio vulnificus* biotype 2. Appl. Environ. Microbiol. **62:**928–935.
32. **Fouz B, Mazoy R, Lemos ML, del Olmo MJ, Amaro C.** 1996. Utilization of hemin and hemoglobin by *Vibrio vulnificus* biotype 2. Appl. Environ. Microbiol. **62:**2806–2810.
33. **Stojiljkovic I, Bäumler AJ, Hantke K.** 1994. Fur regulon in gram-negative bacteria. Identification and characterization of new iron-regulated *Escherichia coli* genes by a Fur titration assay. J. Mol. Biol. **236:**531–545.
34. **Miller JH.** 1972. Experiments in molecular genetics. Cold Spring Harbor Laboratory Press, Cold Spring Harbor, NY.
35. **Amaro C, Biosca EG, Fouz B, Toranzo AE, Garay E.** 1994. Role of iron, capsule, and toxins in the pathogenicity of *Vibrio vulnificus* biotype 2 for mice. Infect. Immun. **62:**759–763.
36. **Esteve-Gassent MD, Fouz B, Amaro C.** 2004. Efficacy of a bivalent vaccine against eel diseases caused by *Vibrio vulnificus* after its administration by four different routes. Fish Shellfish Immunol. **16:**93–105. http://dx.doi.org/10.1016/S1050-4648(03)00036-6.
37. **Amaro C, Fouz B, Biosca EG, Marco-Noales E, Collado R.** 1997. The lipopolysaccharide O side chain of *Vibrio vulnificus* serovar E is a virulence determinant for eel. Infect. Immun. **65:**2475–2479.
38. **Schwyn B, Neilands JB.** 1987. Universal chemical assay for the detection and determination of siderophores. Anal. Biochem. **160:**47–56. http://dx.doi.org/10.1016/0003-2697(87)90612-9.
39. **Andrus CR, Walter MA, Crosa JH, Payne SM.** 1983. Synthesis of siderophores by pathogenic *Vibrio* species. Curr. Microbiol. **9:**209–214. http://dx.doi.org/10.1007/BF01567583.
40. **Arnow LE.** 1937. Colorimetric determination of the components of 3,4-dihydroxyphenyalanine-tyrosine mixtures. J. Biol. Chem. **118:**531–537.
41. **Sambrook J, Russell DW.** 2001. Molecular cloning: a laboratory manual, 3rd ed. Cold Spring Harbor Laboratory Press, Cold Spring Harbor, NY.
42. **Shao CP, Hor LI.** 2000. Metalloprotease is not essential for *Vibrio vulnificus* virulence in mice. Infect. Immun. **68:**3569–3573. http://dx.doi.org/10.1128/IAI.68.6.3569-3573.2000.
43. **Donnenberg MS, Kaper JB.** 1991. Construction of an *eae* deletion mutant of enteropathogenic *Escherichia coli* by using a positive-selection suicide vector. Infect. Immun. **59:**4310–4317.
44. **Biosca EG, Garay E, Toranzo AE, Amaro C.** 1993. Comparison of the outer membrane protein profile of *Vibrio vulnificus* biotypes 1 and 2. FEMS Microbiol. Lett. **107:**217–222. http://dx.doi.org/10.1111/j.1574-6968.1993.tb06033.x.
45. **Laemmli UK.** 1970. Cleavage of structural proteins during the assembly of the head of bacteriophage T4. Nature **227:**680–685. http://dx.doi.org/10.1038/227680a0.
46. **Reed LJ, Muench H.** 1938. A simple method for estimating fifty per cent endpoints. Am. J. Hyg. **27:**493–497.
47. **Lee CT, Pajuelo D, Llorens A, Chen YH, Leiro JM, Padrós F, Hor LI, Amaro C.** 2013. MARTX of *Vibrio vulnificus* biotype 2 is a virulence and survival factor. Environ. Microbiol. **15:**419–432. http://dx.doi.org/10.1111/j.1462-2920.2012.02854.x.
48. **Valiente E, Padrós F, Lamas J, Llorens A, Amaro C.** 2008. Microbial and histopathological study of the vibriosis caused by *Vibrio vulnificus* serovar E in eels: the metalloprotease Vvp is not an essential lesional factor. Microb. Pathog. **45:**386–393. http://dx.doi.org/10.1016/j.micpath.2008.09.001.
49. **Livak KJ, Schmittgen TD.** 2001. Analysis of relative gene expression data using real time quantitative PCR and the $2^{-\Delta\Delta Ct}$ method. Methods **25:**402–408. http://dx.doi.org/10.1006/meth.2001.1262.
50. **Ausubel FM, Brent R, Kingston RE, Moore DD, Seidman JG, Smith JA, Struhl K (ed).** 2007. Current protocols in molecular biology. Wiley-Interscience, New York, NY.
51. **Didelot X, Falush D.** 2007. Inference of bacterial microevolution using multilocus sequence data. Genetics **175:**1251–1266. http://dx.doi.org/10.1534/genetics.106.063305.
52. **Chen CY, Wu KM, Chang YC, Chang CH, Tsai HC, Liao TL, Liu YM, Chen JH, Shen AB, Li JC, Su TL, Shao CP, Lee CT, Hor L-I, Tsai SF.**

2003. Comparative genome analysis of *Vibrio vulnificus*, a marine pathogen. Genome Res. **13:**2577–2587. http://dx.doi.org/10.1101/gr.1295503.
53. **Morrison SS, Williams T, Cain A, Froelich B, Taylor C, Baker-Austin C, Verner-Jeffreys D, Hartnell R, Oliver JD, Gibas CJ.** 2012. Pyrosequencing-based comparative genome analysis of *Vibrio vulnificus* environmental isolates. PLoS One **7:**e37553. http://dx.doi.org/10.1371/journal.pone.0037553.
54. **Kim YR, Lee SE, Kim CM, Kim SY, Shin EK, Shin DH, Chung SS, Choy HE, Progulske-Fox A, Hillman JD, Handfield M, Rhee JH.** 2003. Characterization and pathogenic significance of *Vibrio vulnificus* antigens preferentially expressed in septicemic patients. Infect. Immun. **71:**5461–5471. http://dx.doi.org/10.1128/IAI.71.10.5461-5471.2003.
55. **Roig FJ, Gonzalez-Candelas F, Amaro C.** 2011. Domain organization and evolution of multifunctional autoprocessing repeats-in-toxin (MARTX) toxin in *Vibrio vulnificus*. Appl. Environ. Microbiol. **77:**657–668. http://dx.doi.org/10.1128/AEM.01806-10.
56. **Wang ZG, Wu Z, Xu SL, Zha J.** 2012. Genome sequence of the human-pathogenetic bacterium *Vibrio vulnificus* B2. J. Bacteriol. **194:**7019. http://dx.doi.org/10.1128/JB.01955-12.
57. **Guindon S, Delsuc F, Dufayard JF, Gascuel O.** 2009. Estimating maximum likelihood phylogenies with PhyML. Methods Mol. Biol. **537:**113–137. http://dx.doi.org/10.1007/978-1-59745-251-9_6.
58. **Posada D.** 2008. jModelTest: phylogenetic model averaging. Mol. Biol. Evol. **25:**1253–1256. http://dx.doi.org/10.1093/molbev/msn083.
59. **Akaike H.** 1974. A new look at the statistical model identification. IEEE Trans. Automat. Contr. **19:**716–723. http://dx.doi.org/10.1109/TAC.1974.1100705.
60. **Tamura K.** 1992. Estimation of the number of nucleotide substitutions when there are strong transition-transversion and G+C-content biases. Mol. Biol. Evol. **9:**678–687.
61. **Shimodaira H, Hasegawa M.** 1999. Multiple comparisons of log-likelihoods with applications to phylogenetic inference. Mol. Biol. Evol. **16:**1114–1116. http://dx.doi.org/10.1093/oxfordjournals.molbev.a026201.
62. **Schmidt HA, Strimmer K, Vingron M, von Haeseler A.** 2002. TREE-PUZZLE: maximum likelihood phylogenetic analysis using quartets and parallel computing. Bioinformatics **18:**502–504. http://dx.doi.org/10.1093/bioinformatics/18.3.502.
63. **Strimmer K, Rambaut A.** 2002. Inferring confidence sets of possibly misspecified gene trees. Proc. Biol. Sci. **269:**137–142. http://dx.doi.org/10.1098/rspb.2001.1862.
64. **Foster JT, Beckstrom-Sternberg SM, Pearson T, Beckstrom-Sternberg JS, Chain PS, Roberto FF, Hnath J, Brettin T, Keim P.** 2009. Whole-genome-based phylogeny and divergence of the genus *Brucella*. J. Bacteriol. **191:**2864–2870. http://dx.doi.org/10.1128/JB.01581-08.
65. **Lenski RE, Winkworth CL, Riley MA.** 2003. Rates of DNA sequence evolution in experimental populations of *Escherichia coli* during 20,000 generations. J. Mol. Evol. **56:**498–508. http://dx.doi.org/10.1007/s00239-002-2423-0.
66. **Chase E, Harwood VJ.** 2011. Comparison of the effects of environmental parameters on growth rates of *Vibrio vulnificus* biotypes I, II, and III by culture and quantitative PCR. Appl. Environ. Microbiol. **77:**4200–4207. http://dx.doi.org/10.1128/AEM.00135-11.
67. **Ochman H, Elwyn S, Moran NA.** 1999. Calibrating bacterial evolution. Proc. Natl. Acad. Sci. U. S. A. **96:**12638–12643. http://dx.doi.org/10.1073/pnas.96.22.12638.
68. **Van Ert MN, Easterday WR, Huynh LY, Okinaka RT, Hugh-Jones ME, Ravel J, Zanecki SR, Pearson T, Simonson TS, U'Ren JM, Kachur SM, Leadem-Dougherty RR, Rhoton SD, Zinser G, Farlow J, Coker PR, Smith KL, Wang B, Kenefic LJ, Fraser-Liggett CM, Wagner DM, Keim P.** 2007. Global genetic population structure of *Bacillus anthracis*. PLoS One **2:**e461. http://dx.doi.org/10.1371/journal.pone.0000461.
69. **García K, Gavilán RG, Höfle MG, Martínez-Urtaza J, Espejo RT.** 2012. Microevolution of pandemic *Vibrio parahaemolyticus* assessed by the number of repeat units in short sequence tandem repeat regions. PLoS One **7:**e30823. http://dx.doi.org/10.1371/journal.pone.0030823.
70. **Tanabe T, Naka A, Aso H, Nakao H, Narimatsu S, Inoue Y, Ono T, Yamamoto S.** 2005. A novel aerobactin utilization cluster in *Vibrio vulnificus* with a gene involved in the transcription regulation of the *iutA* homologue. Microbiol. Immunol. **49:**823–834. http://dx.doi.org/10.1111/j.1348-0421.2005.tb03671.x.
71. **Corbeila LB.** 2007. *Histophilus somni* host-parasite relationships. Anim. Health Res. Rev. **8:**151–160. http://dx.doi.org/10.1017/S1466252307001417.
72. **Martínez JL.** 2013. Bacterial pathogens: from natural ecosystems to human hosts. Environ. Microbiol. **15:**325–333. http://dx.doi.org/10.1111/j.1462-2920.2012.02837.x.
73. **Bodilis J, Ghysels B, Osayande J, Matthijs S, Pirnay JP, Denayer S, De Vos D, Cornelis P.** 2009. Distribution and evolution of ferripyoverdine receptors in *Pseudomonas aeruginosa*. Environ. Microbiol. **11:**2123–2135. http://dx.doi.org/10.1111/j.1462-2920.2009.01932.x.
74. **Hantke F.** 1997. Ferrous iron uptake by a magnesium transport system is toxic for *Escherichia coli* and *Salmonella typhimurium*. J. Bacteriol. **179:**6201–6204.
75. **Simon R, Priefer U, Puhler A.** 1983. A broad host range mobilization system for in vivo genetic-engineering transposon mutagenesis in gram-negative bacteria. Biotechnology **1:**787–796.